separations

MDPI

Supplementary Materials

Online Membrane Sampling for the Mass Spectrometric Analysis of Oil Sands Process Affected Water-Derived Naphthenic Acids in Real-World Samples

Joseph Monaghan [1,2], Dylan Steenis [1], Ian J. Vander Meulen [3,4], Kerry M. Peru [4], John V. Headley [4], Chris G. Gill [1,2,5,6] and Erik T. Krogh [1,2,*]

Text S1: Data processing for membrane partitioning of model NAs

Steady-state transport across a capillary hollow fibre membrane is described by Fick's Law with the formula (Crank, 1975; LaPack et al., 1990):

$$F_{SS} = \frac{2\pi L \times K_{PDMS} D_{PDMS}}{\ln\left(\frac{R_o}{R_i}\right)} \times C_{Aq}$$

Where F_{SS} is the flow across the membrane in moles or grams per unit time (to match units of C_{Aq}). The remaining terms can be collected into three groups: (1) geometric terms (length, outer radius [R_o], inner radius [R_i]), (2) permeability terms for the membrane-analyte pair (partition constant [K_{PDMS}], diffusion constant [D_{PDMS}]), and (3) analyte concentration C_{Aq}. Selectivity is derived from the permeability terms, where permeability (P) is defined as the product of the membrane partition constant and diffusion constant:

$$P = K_{PDMS} D_{PDMS}$$

Where D_{PDMS} is inversely related to the natural risetime (τ) of a given analyte across the membrane:

$$D \propto \frac{1}{\tau}$$

We have defined (Duncan et al., 2022) a conditional partition coefficient (K'_{PDMS}) for a given analyte under a specific set of CP-MIMS experimental conditions (flowrate, acceptor phase, membrane geometry) as:

$$K'_{PDMS} = \left(\frac{[Analyte]_{Acceptor}}{[Analyte]_{Donor}}\right) \times \tau$$

Here, we use the relative permeation efficiency (PE; ratio of internal standard corrected calibration slope in aqueous donor phase [4-point] vs. that in the acceptor phase [1-point] within the linear dynamic range) to determine the first term:

$$PE = \frac{slope_{Donor}}{slope_{Acceptor}} = \frac{[Analyte]_{Acceptor}}{[Analyte]_{Donor}}$$

The natural risetime τ is then calculated from signal risetime in response to a step-function increase in concentration in the aqueous donor phase using a pseudo first order model:

$$\ln\left(1 - \frac{S'_t}{S_{SS}}\right)$$

Where S_t, and S_{SS}, are the internal standard and baseline corrected signal intensity at time t, and at steady-state, respectively. A plot of this function over time over 20-90% of the signal rise yields a linear fit where τ is given by the inverse slope. The conditional partition constant K'_{PDMS} appearing in Table 2 results from:

$$K'_{PDMS} = PE \times \tau$$

Note that these conditional partition constants (K'_{PDMS}) are collected under a different set of conditions (flowrate, acceptor phase composition) from Duncan et al. (2022) and will therefore have different absolute values.

Table S1. Summary of m/z included in the 'inclusion list' strategy for OSPW-NAs calibration by CP-MIMS. This list was generated for the 2018 extract of OSPW.

#	*m/z*	R^2	#	*m/z*	R^2	#	*m/z*	R^2
1	181	0.998	14	231	0.999	27	289	0.994
2	183	0.993	15	233	0.998	28	293	0.933
3	193	0.997	16	235	0.999	29	295	0.997
4	195	0.999	17	243	0.999	30	297	0.882
5	197	0.998	18	245	0.999	31	299	0.974
6	207	0.999	19	247	0.998	32	301	0.994
7	211	0.999	20	257	0.997	33	303	0.991
8	215	0.994	21	259	0.999	34	305	0.946
9	217	0.999	22	267	0.991	35	307	0.878
10	219	0.981	23	271	0.997	36	317	0.992
11	221	0.999	24	273	0.998	37	319	0.987
12	223	0.998	25	275	0.994	38	321	0.992
13	229	0.990	26	285	0.993	39	331	0.994

Table S2. Class composition for direct infusion and membrane permeate across 4 OSPW extracts shown in figure 2.

	2018 Extract		2015/1 Extract		2015/2 Extract		2013 Extract	
Class	**Direct Infusion**	**CP-MIMS**	**Direct Infusion**	**CP-MIMS**	**Direct Infusion**	**CP-MIMS**	**Direct Infusion**	**CP-MIMS**
O_2	34.7 ± 0.6	85.9 ± 1.8	62.6 ± 0.9	92.8 ± 0.6	43.7 ± 1.7	87.9 ± 0.8	54.3 ± 0.8	94.8 ± 1.3
O_3	24.4 ± 0.6	4.1 ± 0.8	13.6 ± 0.6	0.7 ± 0.1	21.5 ± 2.8	2.5 ± 0.8	18.9 ± 0.6	2 ± 0.4
O_4	21.1 ± 0.6	0.2 ± 0.2	10.3 ± 0.7	0.1 ± 0	18 ± 2.2	1.8 ± 0.3	16.1 ± 0.6	1.1 ± 0.2
SO_2	5.5 ± 0.2	9.4 ± 0.8	5.4 ± 0.3	6.1 ± 0.2	4.8 ± 0.3	7.1 ± 0.3	1.5 ± 0.1	1.3 ± 0.2
SO_3	7.9 ± 0.2	n.d.[1]	5.4 ± 0.2	n.d.	5.6 ± 0.4	n.d.	6 ± 0.3	n.d.
SO_4	2.3 ± 0.2	n.d.	1.1 ± 0.2	n.d.	2.4 ± 1.6	n.d.	1.3 ± 0.2	n.d.
O_5	2.6 ± 0.2	n.d.	0.8 ± 0.2	n.d.	1.8 ± 0.5	n.d.	1 ± 0.2	n.d.
∑	98.5	99.6	99.2	99.7	97.8	99.3	99.1	99.2

[1]n.d. = no detect

Table S3. Relative calibration slope for various NA mixtures using CP-MIMS with a unit-mass resolution quadrupole-MS.

NA mixture	**Average slope**	**SD**	**O_2-weighted slope**	**SD**	***n***	**Normalized slope**
Sigma-Aldrich	6.5	--	6.9	--	1	0.65
Merichem	10.1	1.0	10.3	1.02	4	1.00
2018 Extract	1.4	0.1	4.1	0.18	3	0.14
2015/1 Extract	1.9	--	3.1	--	1	0.19
2015/2 Extract	1.4	--	3.2	--	1	0.14

Table S4. Evaluation of O_2 contribution to signal intensity at nominal mass resolution for an average of the 4 OSPW extracts shown in Figure 2.

	% O_2					% O_2					% O_2			
m/z	2018 Extract	2015/1 Extract	2015/2 Extract	2013 Extract	*m/z*	2018 Extract	2015/1 Extract	2015/2 Extract	2013 Extract	*m/z*	2018 Extract	2015/1 Extract	2015/2 Extract	2013 Extract
101	**--**	--	--	--	187	100	--	--	--	273	82.3	87.8	89.5	86.7
103	--	--	--	--	189	100	100	--	--	275	71.0	71.1	82.2	75.4
105	--	--	--	--	191	27.4	100	100	55.0	277	62.4	79.5	76.8	72.3
107	--	--	--	--	193	100	100	100	100	279	19.0	27.1	0	17.3
109	--	--	--	100	195	100	100	100	100	281	4.3	8.2	24.7	1.7
111	--	--	--	--	197	100	100	100	100	283	89.4	67.7	96.1	74.6
113	--	--	--	--	199	--	--	--	--	285	92.3	94.7	94.7	93.0
115	--	--	--	--	201	100	100	--	--	287	57.6	67.2	73.2	63.9
117	0	--	--	--	203	93.7	100	100	48.5	289	36.4	36.5	52.4	36.9
119	--	--	--	--	205	100	99	100	100	291	19.3	34.6	56.9	25.7
121	--	--	--	--	207	99.7	100	100	99.9	293	3.1	0	0	0
123	--	--	--	--	209	100	100	100	100	295	16.6	14.5	40.3	7.0
125	0	--	--	--	211	99.7	100	100	100	297	97.3	83	100	90.4
127	--	--	--	--	213	0	0	0	0	299	84.8	87.8	90.7	87.4
129	100	--	--	--	215	97.8	100	100	100	301	31.4	42.9	48.8	38.1
131	--	--	--	--	217	99.3	100	100	100	303	1.6	5.0	0	2.0
133	--	--	--	--	219	98.9	99	100	99.2	305	0	0	5.3	0
135	--	--	--	--	221	99.6	100	99.8	99.8	307	0	0	7.8	0
137	--	--	--	0	223	97.9	99.9	98.7	97.5	309	22.6	7.4	24.7	4.7
139	--	--	--	--	225	2.1	99.1	--	0	311	98.9	97.3	100	98.9
141	--	--	--	--	227	0	0	--	0	313	57.4	76.7	92.0	77.3
143	100	100	100	100	229	99.7	100	100	94.6	315	12.9	20.7	22.6	17.3
145	--	--	--	--	231	98.2	100	100	98.9	317	0	0	0	0.9
147	0	--	0	9.6	233	97.9	99.4	99.2	98.7	319	0	0	0	0
149	0	--	--	0	235	99	99.9	99.5	99.5	321	0	0	35.6	0
151	0	--	--	0	237	94.4	99.9	97.4	98	323	41.9	9.8	3.0	4.3
153	--	--	--	--	239	6.3	22.2	9.0	8.8	325	97.4	100	100	90.5
155	--	--	--	--	241	64	60.7	85.4	59.3	327	34.7	46.8	77.0	39.3
157	--	--	100	100	243	99.9	100	100	100	329	0	0	0	0

159	--	--	--	--	245	95.7	99.3	99	97.8	331	0	0	0	0
161	74.6	--	--	100	247	96.3	97.5	99.1	97.5	333	0	0	0	0
163	0	--	--	0	249	96.8	99.5	99.4	98.3	335	7.3	0	0	0
165	--	--	--	--	251	82.2	96.9	91.6	92.2	337	52.2	0	0	4.1
167	--	--	--	--	253	9.0	18.3	17.9	11.7	339	94.9	100	100	95.5
169	--	100	--	--	255	69.2	64	88.3	65.3	341	16.7	100	--	29.0
171	37.4	--	--	100	257	99.4	100	100	99.9	343	0	0	0	0
173	--	--	--	--	259	92.4	95.4	96.4	94.6	345	0	0	0	0
175	--	--	--	0	261	89.1	91	95.7	92.6	347	14.4	--	0	0
177	0	--	--	100	263	88.4	97	95.7	93.5	349	0	0	0	0
179	0	100	100	40.9	265	42.1	68.1	55.3	51.3	351	6	0	0	1.6
181	100	100	100	100	267	10.6	15.5	64.0	8.5	353	0	--	--	--
183	97.5	100	100	100	269	77.4	66.3	96.4	71.3	355	--	--	--	--
185	100	100	100	100	271	97.7	98.7	99.6	98					

*Channels with known background interference or < 85% O_2 contribution are indicated in red and are excluded from the quantitative comparison shown in figure 5.

Table S5. Summary of quantitative data for archived samples measured by SPE-HRMS and CP-MIMS with a unit mass resolution quadrupole MS.

Sample Name	Class	[NAFCs] by SPE-HRMS[1] (mg/L)	[O_2-NAs] by SPE-HRMS[2] (mg/L)	[O_2-NAs] by CP-MIMS[1] (mg/L)	SD (CP-MIMS; mg/L)	*n* (CP-MIMS)
2021-W-0159	CW-2	22.6	15.3	6.9	0.3	3
2021-W-0327	OSPW	20.6	3.8	1.2	0.5	3
2021-W-0328	OSPW	21.1	3.8	1.2	--	1
2021-W-0329	OSPW	16.9	3.6	1.3	--	1
2021-W-0330	OSPW	19.6	3.7	1.8	--	1
2021-W-0331	CW-2	27.2	7.4	3.4	--	1
2021-W-0332	CW-2	27.2	7.9	3.7	--	1
2021-W-0333	CW-2	24.5	3.7	0.8	0.3	3
2021-W-0334	CW-2	23.5	5.3	1.5	0.3	3
2021-W-0447	CW-1	9.8	5.4	9.8	0.5	3
2021-W-0448	CW-1	7.6	4.8	7.4	--	1
2021-W-0642	CW-1	35.4	22.1	18.3	2.5	3
2021-W-0645	CW-1	41.8	25.8	19.7	2.1	4
2021-W-0662	CW-1	28.5	17.1	23.3	1.4	3
2021-W-0667	CW-1	41.5	22.6	26.9	--	1
2022-W-0095	Env	10.6	1	1.0	--	1
2022-W-0096	Env	94.7	17.1	10.9	--	1
2022-W-0098	Env	30.1	8.8	6.2	--	1
2022-W-0099	Env	28.7	8.7	6.4	0.3	3
2017-415-TowerRoadJH05	Env	3.3	0.1	0.0	--	2
2017-458-JH48	Env	1.1	0	0.0	--	2
2017-460-JH50	Env	7.4	0.3	0.0	0.0	2
2016-A-2097-MRM-DP14	Env	11.1	7.5	8.4	--	1
2017-A-451-JH40	Env	8.6	0.7	0.0	0.1	2
2016-A-2096-RWC-Pump	Env	46.8	24.1	11.7	0.0	2
2017-462-JH52	Env	6.6	0.3	0.2	0.3	3
2016-A-2092-JMP-ETF	Env	26.8	11.5	5.9	0.6	3
2016-A-2098-MRM-ETF	Env	38.2	22	14.0	2.4	3

[1]Reflects weighting by O_2 contribution of calibrant (adjusted $[NA]_T$ = measured $[NA]_T$ × f_{O2}). This results in a factor of 0.347 for CP-MIMS results and 0.745 for SPE-HRMS results.

[2]Calculated as [NAFCs] × f_{O2} from SPE-HRMS data.

Small

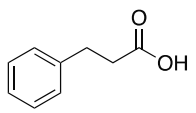

3-phenylpropanoic acid

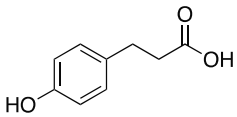

3-(4-hydroxyphenyl) propanoic acid

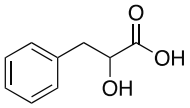

2-hydroxy-3-phenyl propanoic acid

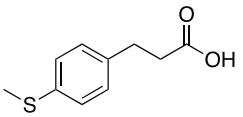

3-(4-methylthiophenyl) propanoic acid

Medium

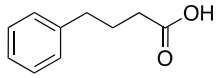

4-phenylbutanoic acid

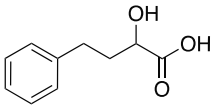

2-hydroxy-4-phenyl butanoic acid

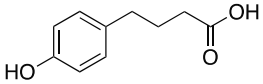

4-(4-hydroxyphenyl) butanoic acid

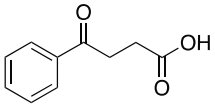

4-keto-4-phenyl butanoic acid

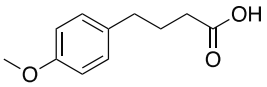

4-(4-methoxyphenyl) butanoic acid

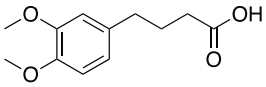

4-(3,4-dimethoxyphenyl) butanoic acid

Large

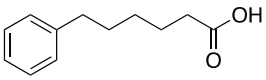

6-phenylhexanoic acid

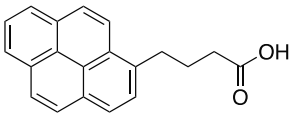

pyrenebutyric acid

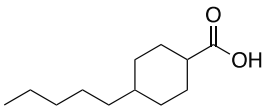

4-pentylcyclohexane carboxylic acid

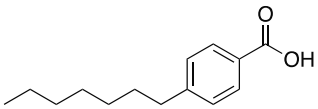

4-heptylbenzoic acid

Figure S1. Structures of model compounds shown employed to evaluate membrane permeability.

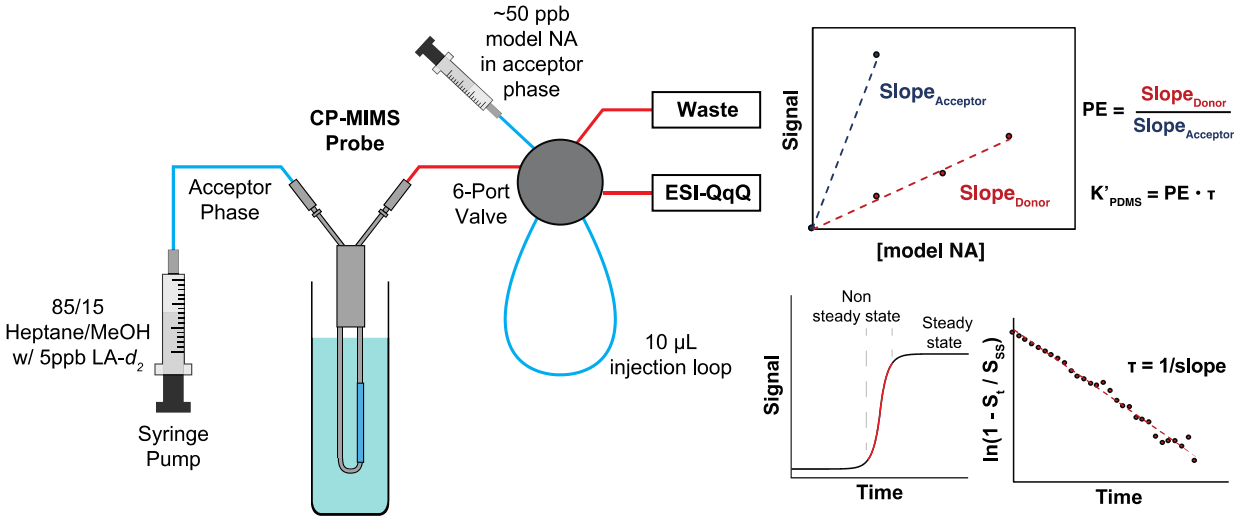

Figure S2. Schematic overview of experimental workflow and data processing to evaluate permeability of model NAs/NAFCs. A calibration curve is measured in both the sample (donor) phase and acceptor phase by spiking model NA into the sample phase or direct infusion, respectively. The permeation efficiency is then taken as the ratio of these two slopes. The natural risetime (τ) is taken as 1/slope of the linearized risetime data (ln[1-Signal$_t$ / Signal$_{SS}$]). The conditional membrane partitioning constant K'$_{PDMS}$ is then calculated as the product of the natural risetime and the permeation efficiency. All permeation studies were performed in triplicate.

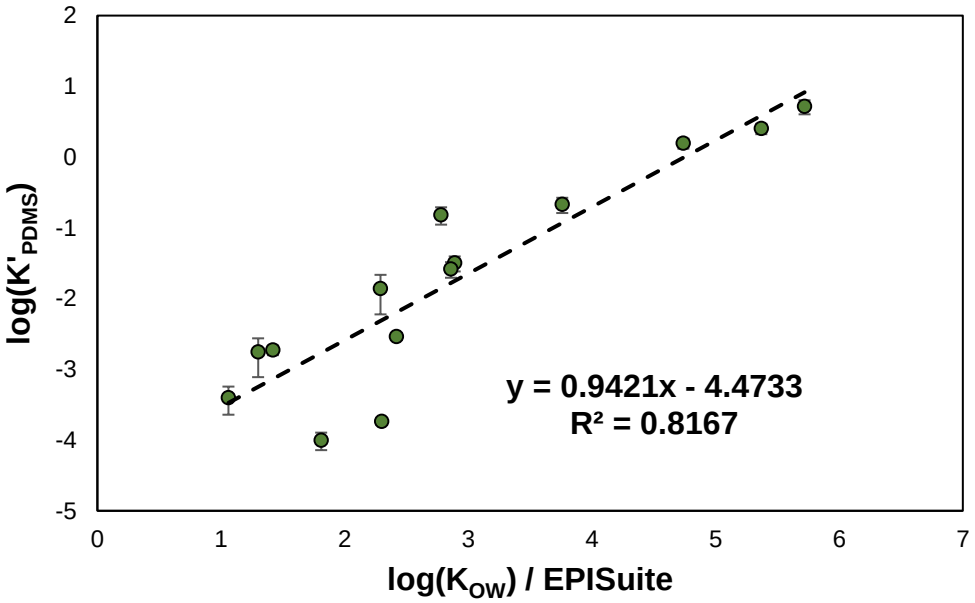

Figure S3. Measured membrane partition coefficient (K'$_{PDMS}$) vs. calculated K_{OW} by EPISuite (Chemspider.com).

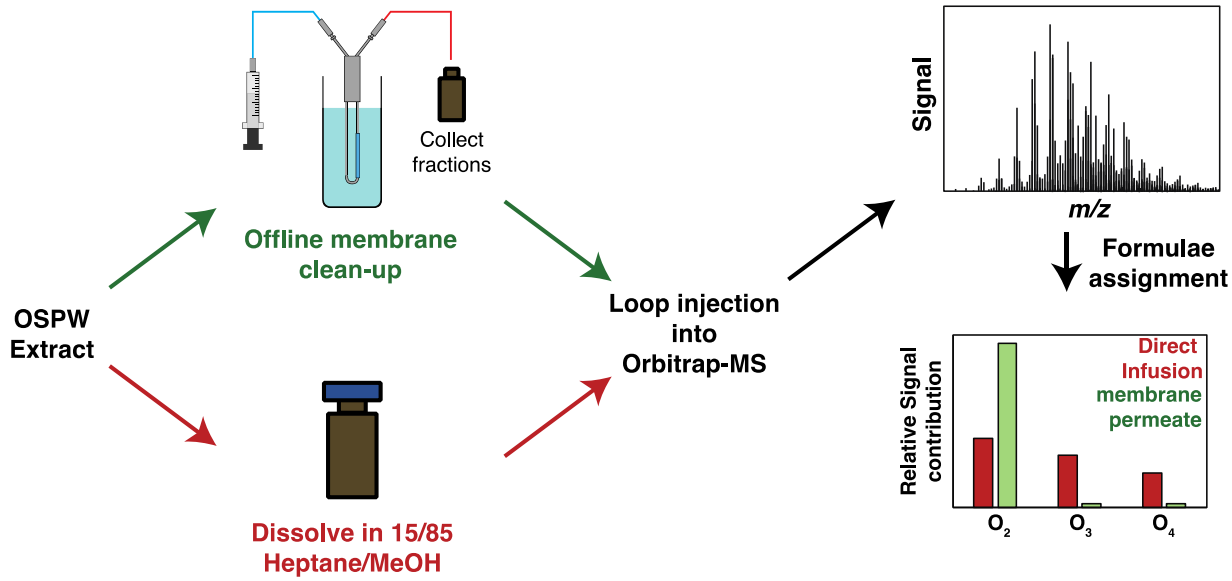

Figure S4. Schematic Overview of experiments evaluating composition OSPW both with (green) and without (red) membrane clean-up. For direct infusion experiments, OSPW extracts are diluted to ca. 2 mg/kg in methanol and loop-injected into the Orbitrap. For the membrane permeate, offline fractions are collected from OSPW extracts spiked into water at ca. 2 mg/L. These fractions are then directly infused into the MS. Formulae assignment was performed using custom Matlab scripts, and then the average signal composition from triplicate injections were averaged. Note that the bar chart does not present data for an actual OSPW, see Figure 3 and Table S2 for the composition of all four OSPW extracts.

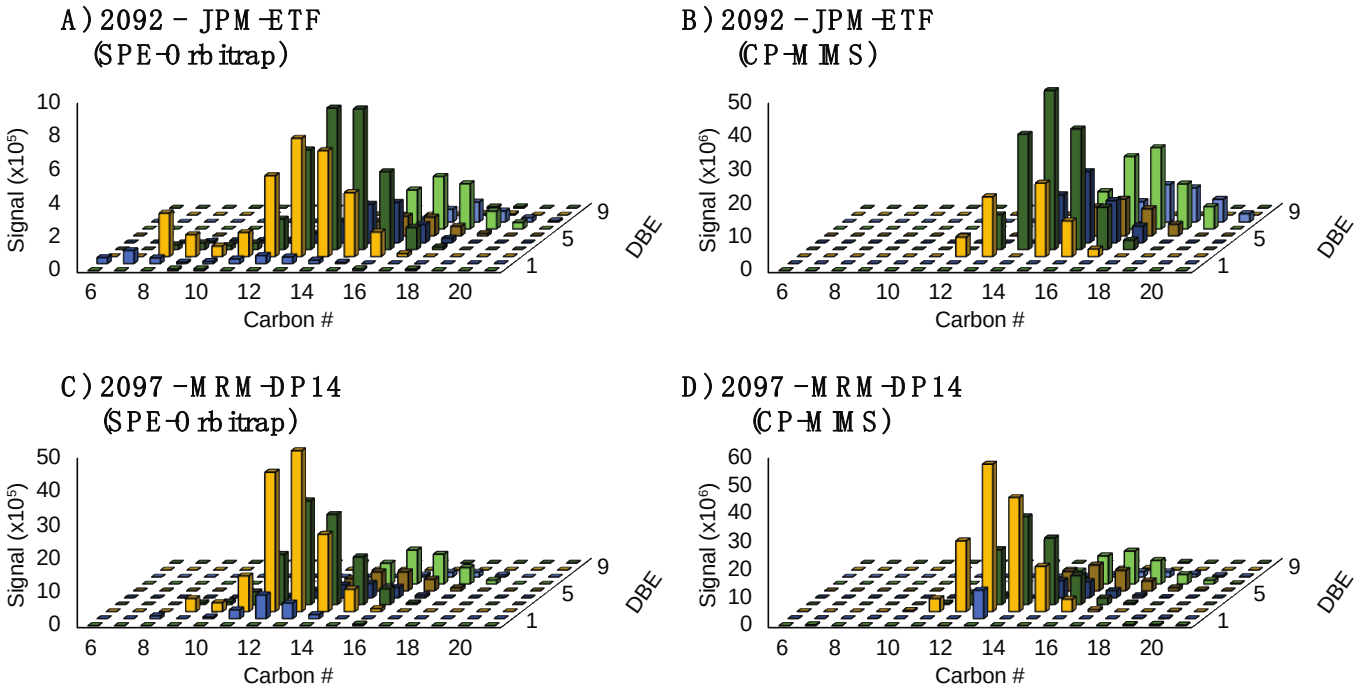

Figure S5. O_2-class distribution for two environmental samples analyzed by SPE-Orbitrap (A & C) and CP-MIMS (B & D). While some differences are observable for minor components of the mixture (possibly due to noise and/or dilution effects), the overall profile is conserved with direct membrane sampling.

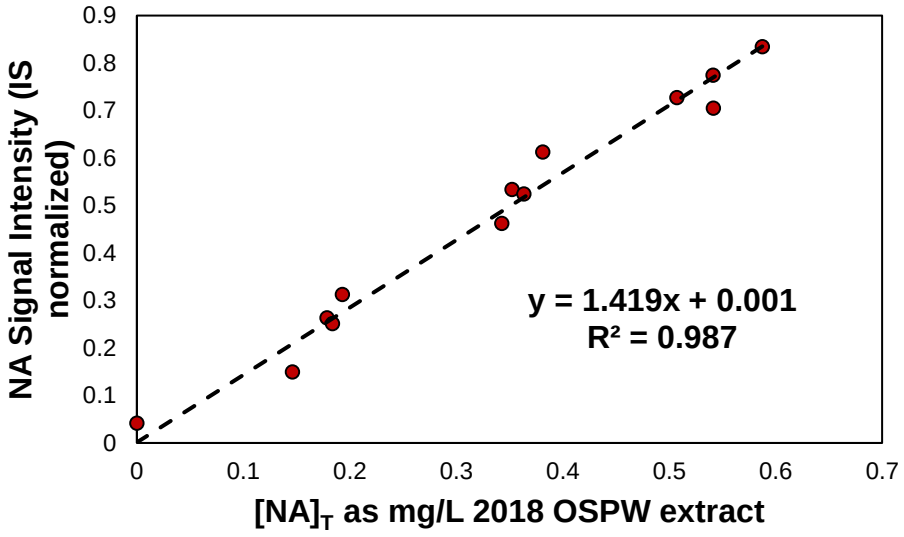

Figure S6. Calibration curve for 2018 OSPW extract of NAs by CP-MIMS with a unit mass resolution quadrupole mass spectrometer.

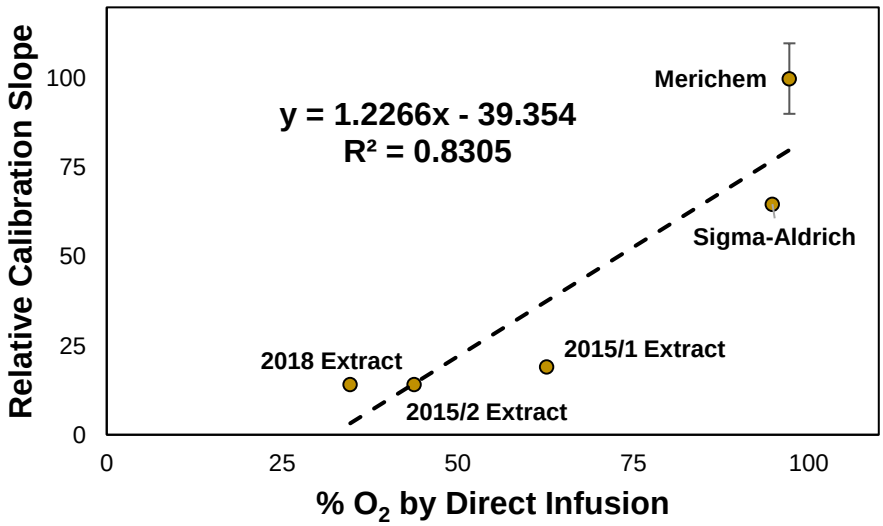

Figure S7. Relative calibration slope (%) using the developed QqQ method versus proportion of O_2-NAs by direct infusion Orbitrap HRMS. Generally, higher O_2 proportions yielded higher relative calibration slopes however the relationship is non-linear, possibly due to differing ionization efficiencies between the mixtures.

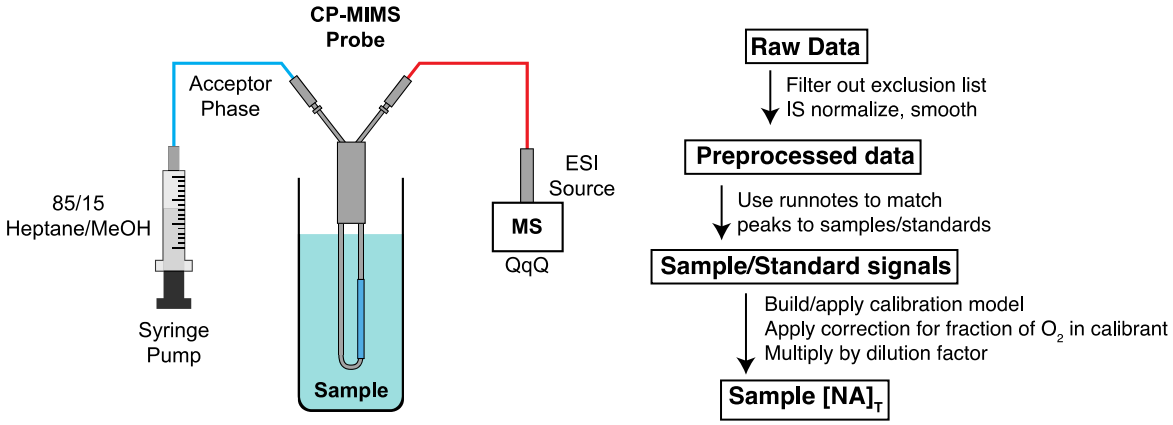

Figure S8. Schematic overview of experimental workflow and data workup for quantitative analysis of real-world samples by CP-MIMS. Samples are acidified to pH < 3 and diluted into the working calibration range of the method. Samples are then measured with the CP-MIMS probe coupled directly to a unit-mass resolution triple quadrupole MS. Raw data is then preprocessed as specified. Signal intensities are extracted from the preprocessed data, and a calibration model is built and applied with the 2018 extract of OSPW. Observed sample concentrations are then adjusted by a factor of 0.347 to compensate for the relative abundance of O_2 NAs in the 2018 extract used as calibrant. Finally, these concentrations are multiplied by the sample dilution factor to output the final quantitative results shown in Figure 5.

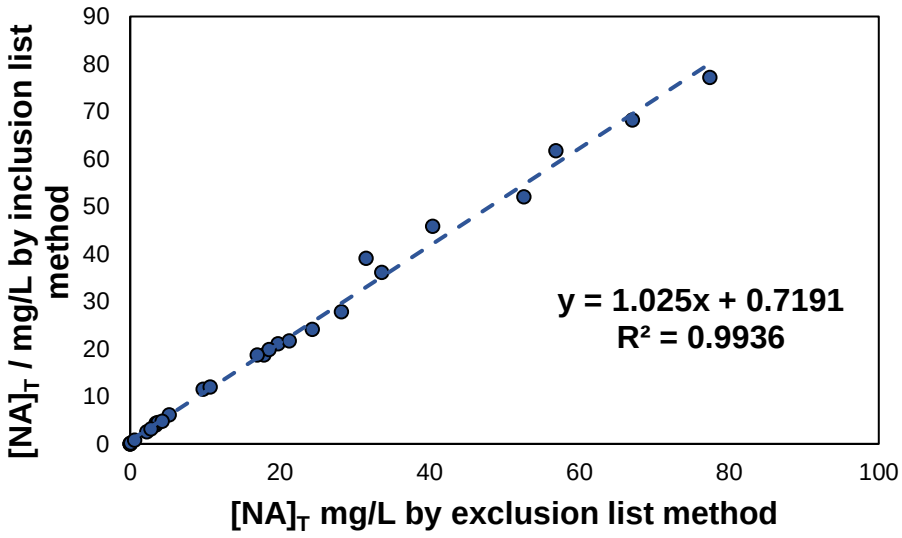

Figure S9. Comparison of quantitation using the 'exclusion list' and 'inclusion list' CP-MIMS methods. Results are generally comparable between the two approaches, however the new 'exclusion list' approach is more adaptable, allowing for direct intercomparison between calibrants (Figure S7). Note that these results are not weighted by the O_2 contribution in the calibrant, as the same calibrant was used for both methods (2018 OSPW extract).

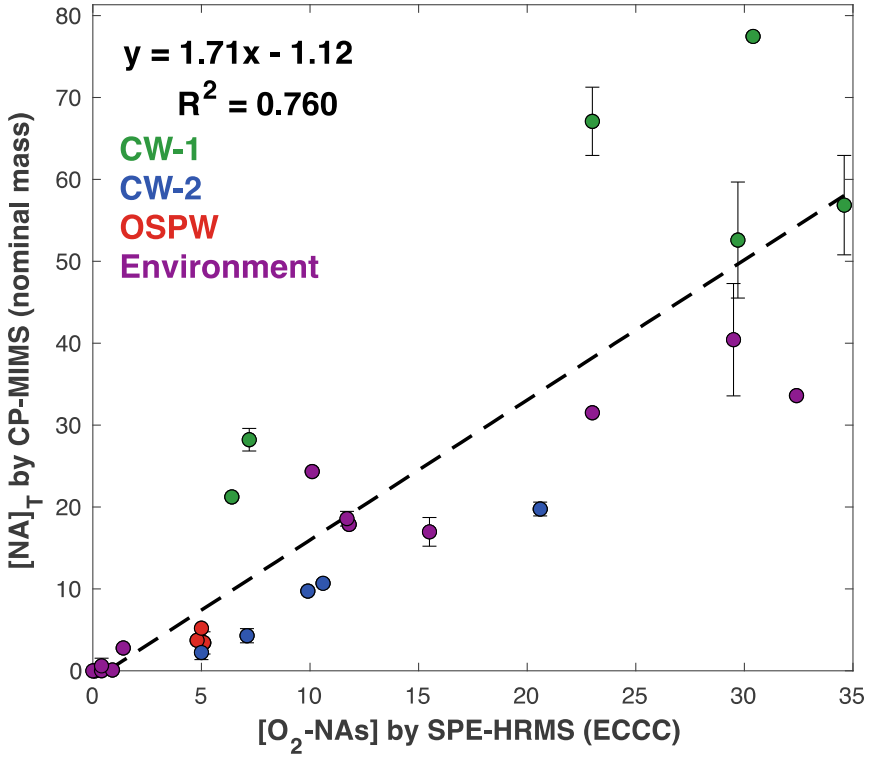

Figure S10. Comparison of un-weighted quantitative results derived from solid-phase extraction high resolution mass spectrometry and CP-MIMS paired to a nominal mass instrument. Quantitative precision on the SPE-HRMS data is estimated at ± 10% from the propagated error of replicate injections and formulae assignment. CP-MIMS results appear positively biased due to the lower O_2 contribution present in the 2018 extract employed (34.7% vs. 74.5% in the SPE-HRMS calibrant).

References:

Chemspider. Chemspider. 2022. Royal Society of Chemistry.

Crank J. The Mathematics of Diffusion. London: Oxford University Press, 1975.

Duncan KD, Hawkes JA, Berg M, Clarijs B, Gill CG, Bergquist J, Lanekoff I, Krogh ET. 2022. Membrane Sampling Separates Naphthenic Acids from Biogenic Dissolved Organic Matter for Direct Analysis by Mass Spectrometry. Environ Sci Technol. 56, 3096-3105. 10.1021/acs.est.1c07359

LaPack MA, Tou JC, Enke CG. 1990. Membrane mass spectrometry for the direct trace analysis of volatile organic compounds in air and water. Analytical Chemistry. 62, 1265-1271. 10.1021/ac00212a013